DEVELOPMENT OF ADVANCED STABILITY THEORY SUCTION PREDICTION TECHNIQUES FOR LAMINAR FLOW CONTROL

Andrew J. Srokowski
NASA Langley Research Center

SUMMARY

The problem of obtaining accurate estimates of suction requirements on swept laminar flow control wings is discussed. A fast accurate computer code developed to predict suction requirements by integrating disturbance amplification rates is described. Assumptions and approximations used in the present computer code are examined in light of flow conditions on the swept wing which may limit their validity.

INTRODUCTION

The development of viable laminar flow control technology requires consideration of aerodynamics, structures, and maintainability. Advancements in aerodynamics and structures since the X-21 project of the early/middle sixties together with the projected world fuel supply/price situation have resulted in new efforts to develop laminar flow control (LFC) technology for subsonic CTOL transports (ref. 1). Both the aerodynamic and structural considerations in the design of an LFC transport are impacted by the gross amount and detailed distribution of the suction air flow required for laminar flow. The problem of predicting required suction flow rates on swept LFC wings has received little attention in the past 10 years. In this time span, new powerful computers and numerical techniques have evolved which permit the development of practical suction prediction methods using advanced boundary-layer stability theories. (See refs. 2 to 4.) The more sophisticated theories account better for the real-life physics of the boundary-layer stability/transition problem (ref. 5), and thus, allow a higher confidence level in the predicted suction rates for wing configurations and pressure distributions which may be considerably different from those for which experimental data are currently available.

This paper includes (1) a brief look at the physics of the transition problem; (2) a short review of prior methods for determining suction flow rates on swept LFC wings; (3) a general description of the present updated method and computer code and finally (4) other effects not accounted for in the present method, their relative importance, and regions of the swept wing for which they may have to be considered in future suction prediction techniques.

SYMBOLS

c	wing chord taken parallel to free-stream direction
C_p	pressure coefficient, $\frac{p - p_\infty}{0.5\rho_\infty U_\infty^2}$
L	length scale
N	natural logarithm of the ratio of a boundary-layer disturbance amplitude to its amplitude at neutral stability.
n	crossflow boundary-layer velocity component (perpendicular to local potential velocity)
p	static pressure
R	local length scale Reynolds number, $\frac{\rho_e U_e L}{\mu_e}$
r	radial distance to chord line in conical wing approximation
R_n	crossflow Reynolds number, $\frac{\rho_e n_{max} \delta_{0.1n_{max}}}{\mu_e}$, where $\delta_{0.1n_{max}}$ is the height at which the crossflow velocity attains 10% of its maximum value (point furthest from the surface)
R_t	tangential or streamwise Reynolds number, $\frac{\rho_e t_e \theta}{\mu_e}$
s	surface distance
t	streamwise or tangential boundary-layer velocity component (parallel to local potential velocity)
u_o	component of boundary-layer velocity in direction normal to radial boundary-layer coordinate
U	total velocity
v	component of boundary-layer velocity normal to surface
V_G	group velocity
w_o	component of boundary-layer velocity along radial boundary-layer coordinate
x	distance in chord direction

y	distance normal to surface
α	nondimensional wavenumber in u_0 direction (see figs. 4 and 5), $\frac{2\pi L}{\lambda_{u_0}}$
β	nondimensional wavenumber in w_0 direction, $\frac{2\pi L}{\lambda_{w_0}}$
δ	boundary-layer thickness
θ	boundary-layer momentum thickness of t profile
μ	viscosity
ρ	density
χ	crossflow Reynolds number, $\frac{\rho_e n_{max} \delta}{\mu_e}$
ψ	angle of line that is normal to the disturbance wavefront, $\tan^{-1}(\beta/\alpha)$; also perturbation stream function (eq. (5) and (6))
ω	nondimensional complex frequency

Subscripts

e	local potential flow
i	imaginary part
max	maximum
min	minimum
r	real part
W	wall
∞	free stream

PHYSICS OF THE STABILITY/TRANSITION PROBLEM

A simple visualization of the flow development on a flat plate would include sequentially an initial laminar linear region, a laminar nonlinear region, a transitional nonlinear region, and finally, turbulent flow. The relative length of the pre-turbulent regions depends to a significant extent on a multitude of factors such as surface roughness, free-stream noise and vorticity, and pressure gradient. Any of these factors, if strong enough, may cause some of the preturbulent region to be shortened or bypassed. A detailed discussion of such phenomena may be found in the literature (refs. 5 and 6).

For a laminar boundary layer exposed to relatively weak external disturbances, small disturbances undergo linear amplification. In two-dimensional incompressible flow, the disturbance waves which are amplified the most are those moving in the direction of the external flow (two-dimensional waves). They are due to viscous instability of the boundary layer (refs. 7 and 8).

The situation on a swept wing is complicated by the presence of boundary-layer crossflow. (See refs. 9 and 10.) Figure 1 indicates that near the leading and trailing edges of a swept wing, the slow moving fluid elements in the boundary layer close to the surface are more strongly deflected by the pressure gradients than fluid elements nearer to the edge of the boundary layer. Figure 2 illustrates the resulting boundary-layer profiles. The crossflow profile has an inflection point which is strongly destabilizing (inflexional instability). Thus, on a swept wing there are normally two types of instabilities: the viscous or Tollmien-Schlichting instability and the inflexional or crossflow instability. Figure 3 illustrates the stabilizing effect of suction on these profiles. This effect results from a thinning and alteration of the boundary-layer profile, and also, in the case of the crossflow instability, stronger damping when the inflexion point is brought nearer to the surface. If suction is strong enough, complete stabilization will result with all boundary-layer disturbances being damped. However, this condition would mean excessive suction rates with corresponding system penalties. (See ref. 11.) A more efficient design is to use suction rates and distributions which would allow disturbance growth to the point of incipient transition. The points that have been discussed so far are not new and have been known for the past 10 to 20 years. What is new is the methodology being developed to compute the amount and distribution of suction that will allow disturbances on a swept wing to grow to the point of incipient transition. This will be discussed after a brief review of some previous methods for swept LFC wings.

PREVIOUS METHODS

The method of direct integration of disturbance amplification rates obtained from linear/parallel stability theory computations has been recently used extensively for problems involving axisymmetric bodies in water (ref. 12). However, for the three-dimensional swept-wing problem, local methods have traditionally been used (ref. 13). By local is meant that at selected points along the chord, a flow quantity is examined, and flow stability evaluated solely from an experimental correlation involving that local quantity. One such method is known as the χ method (ref. 14).

In figure 2 there is a maximum crossflow velocity inside the viscous boundary layer. This velocity together with the boundary-layer thickness can be used to form a Reynolds number called the crossflow Reynolds number or χ. For a given experimental airfoil pressure distribution, χ can be calculated along the chord, and the value of χ obtained which corresponds to the physical transition location. A correlation is then obtained between allowable χ values and the extent of laminar flow. The idea is to apply suction to keep χ below a certain critical value so that laminar flow is not lost due to crossflow instability. The problem with this method is that the local crossflow Reynolds

number does not contain any information at all about the disturbance amplification history of the boundary layer which is vital to reliable transition predictions (ref. 5). Wing configurations and pressure distributions significantly different from those used in the correlation may have different levels of χ at transition.

Another local method is known as the X-21 method and was used to determine X-21 suction rates and distributions (ref. 15). This method incorporates stability calculations, but in a local sense. What is done is that the streamwise and crossflow boundary-layer profiles on a swept wing are first normalized in an appropriate fashion and neutral stability curves are then obtained from linear, parallel stability theory. Neutral stability means that condition where boundary-layer disturbances are neither amplified nor damped. The so-called crossflow and streamwise minimum critical Reynolds number ($R_{n,min}$ and $R_{t,min}$, respectively) obtained from neutral stability curves are then related to the second derivative of the appropriate velocity profile (streamwise or crossflow).

The relations that were obtained are (from ref. 15):

$$\text{Crossflow} \quad R_{n,min} = 60 - 0.7 \left(\frac{\partial^2 (n/n_{max})}{- \partial \left(y/\delta_{0.1n,max} \right)^2} \right) \tag{1}$$

$$\text{Streamwise} \quad (R_{t,min})^{1/3} = 6 - 127 \left(\frac{\partial^2 (t/t_e)}{\partial (y/\theta)^2} \right) \tag{2}$$

where n and t are the crossflow and streamwise velocities, respectively, (see fig. 2), y is distance normal to the surface, θ is the streamwise momentum thickness, and $\delta_{0.1n_{max}}$ is the distance above the surface where the crossflow velocity is 10 percent of its maximum value. These relations are valid only for the class of boundary-layer profiles for which they were derived. Additionally, they only track neutral stability.

For the X-21 suction predictions, it was necessary to obtain an idea of the margin by which computed neutral stability Reynolds numbers might be exceeded. This was done by comparison with experiment and it was found that the crossflow Reynolds numbers could be exceeded by about 80 percent and the streamwise criterion by 200.

This comparison results in the following criteria:

$$R_{n,max} = 1.8 \, R_{n,min} \tag{3}$$

$$R_{t,max} = R_{t,min} + 200 \tag{4}$$

Numerous examples of the use of these criteria may be found in the literature (refs. 15 to 18).

The obvious advantage of local methods such as these is that they are easy to apply and do not consume large amounts of computer time. The obvious disadvantage is, of course, the confidence level of these methods. They do not account in any way for the disturbance growth history, which is a necessary part of a rational transition prediction method. Thus, it may be dangerous to rely exclusively on such methods for wing configurations and pressure distributions which depart significantly from those used in their calibration.

The ideal advanced method should account for as much of the physics as possible, should not require an inordinate amount of computer time, and finally, should be user oriented with relative ease of operation. The method to be described in the following section was developed with these goals in mind.

PRESENT METHOD

Description

The present method is designed to compute the incompressible stability characteristics of laminar compressible boundary layers on swept, tapered wings with suction. The boundary-layer profiles are computed by program MAIN (ref. 19). Program MAIN is laminar, compressible, with adiabatic wall and wall suction boundary conditions. Taper effects are incorporated by assuming that the wing can be represented as part of a semi-infinite conical surface. The assumption of conical similarity then allows the results of a computation at one spanwise position to be simply scaled to obtain boundary-layer profiles at any other spanwise station. Boundary-layer computations are made along an arc of constant radius (r). Wing geometry and surface pressures are specified along a chordline parallel to the free stream which intersects the arc of constant radius at the leading edge. Figure 4 indicates these relationships.

The results of program MAIN are input into stability program SALLY, which performs incompressible, linear, and parallel stability computations. SALLY solves the Orr-Sommerfeld equation:

$$\left(\frac{d^2}{dy^2} - \alpha^2 - \beta^2\right)^2 \psi = iR\left\{(\alpha u_0 + \beta w_0 - \omega) \cdot \left[\frac{d^2}{dy^2} - \alpha^2 - \beta^2\right]\psi - \left(\alpha \frac{\partial^2 u_0}{\partial y^2} + \beta \frac{\partial^2 w_0}{\partial y^2}\right)\psi\right\} \tag{5}$$

where the quantity ψ is the perturbation stream function with boundary conditions

$$\psi(0) = \frac{\partial \psi}{\partial y}(0) = 0 \quad (\psi(\infty) \text{Bounded}) \tag{6}$$

α, β are the wave number components of the disturbance, ω is the complex disturbance frequency, u_o and w_o are mean flow velocity components, and R is the Reynolds number. (See fig. 4.)

A spectral technique involving Chebyshev polynominals is used to obtain solutions to this equation. This solution technique has the advantages of high accuracy combined with computational speed and efficiency. Details of the solution procedure are available in reference 2.

SALLY obtains at each chordwise computational station for given wavenumber components α, β, the frequency of the disturbance ω_r, the disturbance amplification rate ω_i, and the group velocity vector V_G where ω_r and ω_i are the real and imaginary parts of ω in equation (5). This information is used to determine the integrated disturbance amplitude ratio in the following manner. First, the frequency of the disturbance that is to be followed is specified, and SALLY proceeds from station to station along the chord until an instability of the required frequency is detected. An iteration is then performed to obtain the wave of maximum amplification at that frequency. This amplification rate is then integrated to the next station (see fig. 5) along the surface distance determined by the direction of the group velocity vector. In addition to determining the direction of integration, the group velocity is used to convert temporal amplification rates obtained from the stability solution to the spatial amplification rates that are actually integrated. Thus, at each station, the amplitude ratio of the disturbance is available. The logarithm of this ratio gives the so-called "N-factor" of the disturbance. A detailed discussion of the present mehtod may be found in reference 20.

Figure 6 illustrates schematically how disturbance growth information can be used to determine suction rates. Assume that an airfoil (without suction) is placed in a wind tunnel, and surface pressures and transition location are determined. The surface pressures and wing geometry are used by program MAIN to compute the boundary-layer profiles which are input to the SALLY stability code. SALLY computes integrated disturbance growth along the chord, and the growth "N factor" at the transition location is determined. If suction is now applied to the surface of the wing so that it is below the disturbance growth factor corresponding to transition, then laminar flow should be maintained. Thus, the first task is to determine allowable disturbance growth factors. This is done by calibration with experiment.

Calibration

Since transition is affected by factors such as free-stream noise and turbulence, calibration of a transition prediction method should involve data

in a low disturbance environment. For this reason data obtained in the Ames 12-foot tunnel was used (refs. 21 and 22). This question will be discussed only briefly here, and the reader is referred to reference 20 for more detail. Figure 7 illustrates the calibration process. Results are shown for two separate experimental investigations in the Ames 12-foot tunnel. One investigation involved an unsucked two-dimensional wing section at various sweeps and Reynolds numbers; the other was a two-dimensional 30° swept wing with suction through spanwise slots. The procedure then is to obtain boundary-layer profiles with program MAIN for the test Mach number and pressure distribution. These profiles are input to SALLY and the disturbance growth N-factor corresponding to the experimentally observed transition location is obtained. Figure 7 gives an example of such a calibration for stationary crossflow disturbances. The curves marked 40B and 40C do not have a transition location because transition occurred forward of the first measuring station at 20 percent chord. Note that the N-factors for the other curves at transition fall in a band $9.5 \lessapprox N \lessapprox 11$. This then gives an indication of allowable crossflow disturbance growth for laminar flow over the front part of the wing. It turns out that three separate calibrations need to be carried out: (1) front part of wing crossflow; (2) mid-chord Tollmien-Schlichting (streamwise disturbances); and (3) rear part of wing crossflow. This aspect will not be addressed here, and the reader is again referred to reference 20. Reference 22 indicates that suction was adjusted on the wing of that experiment so that laminar flow would be maintained along the entire chord with minimum suction flow rates. Note that maximum growth factors obtained for the suction case S2 fall within the range of N factors at transition.

Sample Application

Figure 8 shows the pressure distribution over the upper and lower surface of an LFC applicable supercritical wing section for a design shockless condition. Note the large supercritical region on the upper surface and the very small region of supercritical flow along the lower surface. Figure 9 shows two suction distributions for the upper surface of the airfoil of figure 8. Note the higher suction rates at the front and rear for control of the crossflow, and the relatively low mid-chord suction for control of streamwise Tollmien-Schlichting disturbances. The solid suction curve corresponds to a suction level that allows the highest possible disturbance growth without exceeding established growth limits. This suction distribution should maintain laminar flow to 100 percent of the chord. Figure 10 shows the corresponding crossflow growth factors; solid and dashed curves of figure 10 corresponding to those of figure 9. The dashed curve represents a slightly lower suction level with the result that the solid curve limit is exceeded by about 84 percent chord. This indicates that full-chord laminar flow cannot be maintained with the lower suction level.

Status

The SALLY stability code is operational with

(a) Typical run times: 3 minutes on Control Data CDC 6600 for one spanwise station

(b) 160,000 octal words of storage

Improvements forthcoming are

(a) 40 percent decrease in memory requirements

(b) 45 percent decrease in run times.

OTHER EFFECTS

The assumptions contained in SALLY are that (1) it is incompressible, (2) it is linear, (3) it is parallel, and (4) it has no wall curvature terms. These assumptions are now considered and the flow situations on the wing for which they may have limited validity are examined.

Compressibility

From figure 8 it can be seen that a significant portion of the upper surface is in a region of locally supercritical flow. Although the profiles used by SALLY are generated by a compressible boundary-layer program, SALLY itself solves the incompressible stability equations. So the question is, how much of an error is incurred by using incompressible stability for wings with significant supercritical regions. Figure 11 gives a comparison between compressible and incompressible growth rates for Tollmien-Schlichting (streamwise) disturbances in the upper surface supercritical region of the wing of figure 8. Calculations performed by L. Mack of Jet Propulsion Laboratory (unpublished) indicate that compressibility decreases the local disturbance growth rates and, in addition, it changes the bandwidth of unstable frequencies. Incompressible calculations in supercritical regions would therefore tend to be conservative (and would estimate higher suction rates). It turns out that the crossflow disturbances are dominant in the lower Mach number regions of the flow and calculations for the upper surface of the configuration of figure 8 indicate about a 10 percent decrease in growth rates due to compressibility. Since most of the suction is needed to control crossflow (see fig. 9), it is seen that compressibility effects will not significantly change the total required suction flow, but may be important in determining the details of the suction distribution. Also, because of the low local pressure levels in the supercritical region, the compressibility effects may have a sizeable favorable influence upon the pumping power.

Nonparallel Effects

The assumption of parallel flow in the equations used in SALLY may be violated to some extent. For example, figure 12 shows that in the region in the near vicinity of the slot, streamlines diverge, and the flow is obviously not parallel. How important this effect is has not yet been established. Figure 13 gives an example of the type of calculation (obtained from A. Nayfeh of Virginia Polytechnic Institute and State University) that can only be done accurately by including nonparallel effects. A flat plate, six units long, is placed in a stream of Mach number 0.8, and the integrated growth of a disturbance of nondimensional frequency 1×10^{-5} is determined for a number of suction conditions on the plate. All growth factor levels shown are at the end of the plate. If a given total suction is distributed evenly along the plate, a growth factor of slightly over 4.5 is obtained. If the total suction amount is kept fixed but now distributed only over the first half of the plate, the growth factor goes up to almost 8. Further concentration of the suction results in growth factors which start to approach those obtained with no suction (level indicated by top bar). Increasing suction concentration results in increasing severity of nonparallel flow in the region where suction terminates. A series of alternate suction no-suction strips approximates the real life case of suction through spanwise slots. Also, however, if many fine slots are used, the nonparallel and "solid surface" effects, as shown on figure 13, are probably not very severe, since continuous suction would be approached. When such nonparallel calculations are performed, they may reveal that certain critical slot spacings will result in a resonance phenomenon greatly increasing the normal amplification rates of particular frequencies of streamwise Tollmien-Schlichting disturbances.

Nonlinear Effects

Use of linearized stability equations assumes that growth rates of any wave can be calculated independently of the growth of any other wave. In certain situations, this may not hold. Figure 14 illustrates three situations where nonlinear effects may be important. First, waves may grow to amplitudes where streamwise and crossflow type disturbances begin to interact with each other. Second, although wings will ideally be designed for shockless conditions, off-design shocks will occur and may result in sufficiently rapid mean flow changes to cause nonlinear effects to become important. A third possibility is that the suction slots themselves may induce disturbances sufficient to make nonlinear effects important.

Wall Curvature Effects

It is known that in regions of concave curvature, such as on the lower surface of the wing of figure 8, a centrifugal instability known as Taylor-Goertler instability will occur (ref. 23). These are vortex type instabilities and are due solely to centrifugal effects. New computational stability codes are being developed which will have the capability of computing Taylor-Goertler instabilities quickly and accurately.

CONCLUDING REMARKS

An advanced three-dimensional boundary-layer stability code has been developed to optimize LFC suction requirements. A new version 45 percent faster and requiring 40 percent less computer storage will soon be available. Compressibility effects have been found to be important in the sense that they will impact the details of the suction distribution. The importance of non-parallel, nonlinear, and Taylor-Goertler effects is being investigated.

REFERENCES

1. Sturgeon, R. F.; Bennett, J. A.; Etchberger, F. R.; Ferrill, R. S.; and Mead, L. E.: Study of the Application of Advanced Technologies to Laminar-Flow Control Systems for Subsonic Transports. Volume I: Summary. NASA CR 144975, 1976.

2. Benney, David J.; and Orszag, Steven A.: Stability Analysis for Laminar Flow Control - Part 1. NASA CR-2910, 1977.

3. Saric, William S.; and Nayfeh, Ali Hasan: Nonparallel Stability of Boundary Layers With Pressure Gradients and Suction. Laminar-Turbulent Transition, AGARD-CP-224, May 1977.

4. Hocking, L. M.: Non-Linear Instability of the Asymptotic Suction Velocity Profile. Quart. J. Mech. & Appl. Math., vol. XXVIII, pt. 3, Aug. 1975, pp. 341-353.

5. Reshotko, Eli: Stability Theory as a Guide to the Evaluation of Transition Data. AIAA J., vol. 7, no. 6, June 1969, pp. 1086-1091.

6. Morkovin, Mark V.: Critical Evaluation of Transition From Laminar to Turbulent Shear Layers With Emphasis on Hypersonically Traveling Bodies. AFFDL-TR-88-149, U.S. Air Force, Mar. 1969. (Available from DDC as AD 686 178.)

7. Mack, L. M.: Boundary Layer Stability Theory. 900-277 Rev. A (Contract No. NAS 7-100) Jet Propulsion Lab., California Inst. Technol., Nov. 1969.

8. Betchov, R.; and Criminale, William O., Jr.: Stability of Parallel Flows. Academic Press, Inc., 1967.

9. Pfenninger, W.: Flow Problems of Swept Low-Drag Suction Wings of Practical Construction at High Reynolds Numbers. Ann. N.Y. Acad. Sci., vol. 154, art. 2, Nov. 22, 1968, pp. 672-703.

10. Schlichting, Hermann (J. Kestin, trans.): Boundary-Layer Theory. Sixth ed., McGraw-Hill Book Co., Inc., c.1968.

11. Pfenninger, W.: Some General Considerations of Losses in Boundary Layer Suction Ducting Systems. Rep. BLC-29, Northrop Corp., Feb. 1954.

12. Scotti, R. S.; and Corbett, K. T.: Laminar Body Analysis Heat Plus Suction Stabilized. ONR-CR289-013-1F, U.S. Navy, Dec. 1976. (Available from NTIS as AD-A040396.)

13. Hirschel, E. H.: Theoretical Investigation of Transition Phenomena in the Boundary Layer on an Infinite Swept Wing. DGLR Paper No. 72-124, Symposium on Aerodynamics of Airfoils in Transonic Flow, Oct. 1972.

14. Owen, P. R.; and Randall, D. G.: Boundary Layer Transition on a Sweptback Wing: Tech. Mem. Aero 277, British R.A.E., May 1952.

15. LFC Aircraft Design Data Laminar Flow Control Demonstration Program. Final Report. NOR-67-136 (AF 33/657-13930), Northrop Corp., June 1967. (Available from DDC as AD-819317.)

16. Summary of Laminar Boundary Layer Control Research. Vol. II, ASD-TDR-63-554, U.S. Air Force, Mar. 1964. (Available from DDC as AD 60586.)

17. Gross, L. W.: An Analysis of the Boundary Layer Development on a 30° Swept Laminar Suction Wing. Rep. BLC-134 (NAI-61-244), Northrop Corp., 1962.

18. Pfenninger, W.: USAF and Navy Sponsored Northrop LFC Research Between 1949 and 1967 and Design Considerations of Large Global Range High Subsonic Speed LFC Transport Airplanes. Presented at the AGARD/VKI Special Course on "Concepts for Drag Reduction." (Rhode-St-Genese, Belgium), Mar. 28-Apr. 1, 1977.

19. Kaups, Kalle; and Cebeci, Tuncer: Compressible Laminar Boundary Layers With Suction on Swept and Tapered Wings. J. Aircraft, vol. 14, no. 7, July 1977, pp. 661-667.

20. Srokowski, A. J.; and Orszag, S. A.: Mass Flow Requirements for LFC Wing Design. AIAA Paper No. 77-1222, Aug. 1977.

21. Boltz, Frederick W.; Kenyon, George C.; and Allen, Clyde Q.: Effects of Sweep Angle on the Boundary-Layer Stability Characteristics of an Untapered Wing at Low Speeds. NASA TN D-338, 1960.

22. Gault, Donald E.: An Experimental Investigation of Boundary-Layer Control for Drag Reduction of a Swept-Wing Section at Low Speed and High Reynolds Numbers. NASA TN D-320, 1960.

23. Tobak, M.: On Local Goertler Instability. ZAMP, vol. 22, 1977, pp. 130-143.

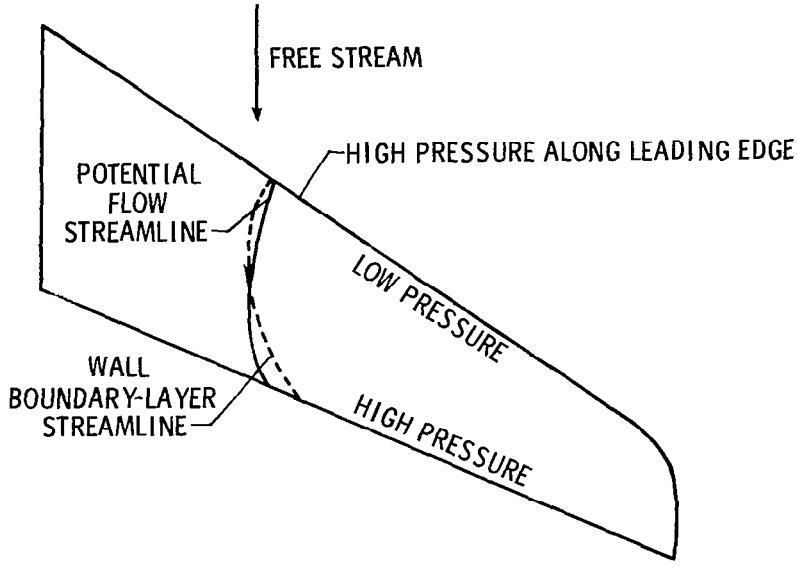

Figure 1.- Flow conditions on typical sweptback wing.

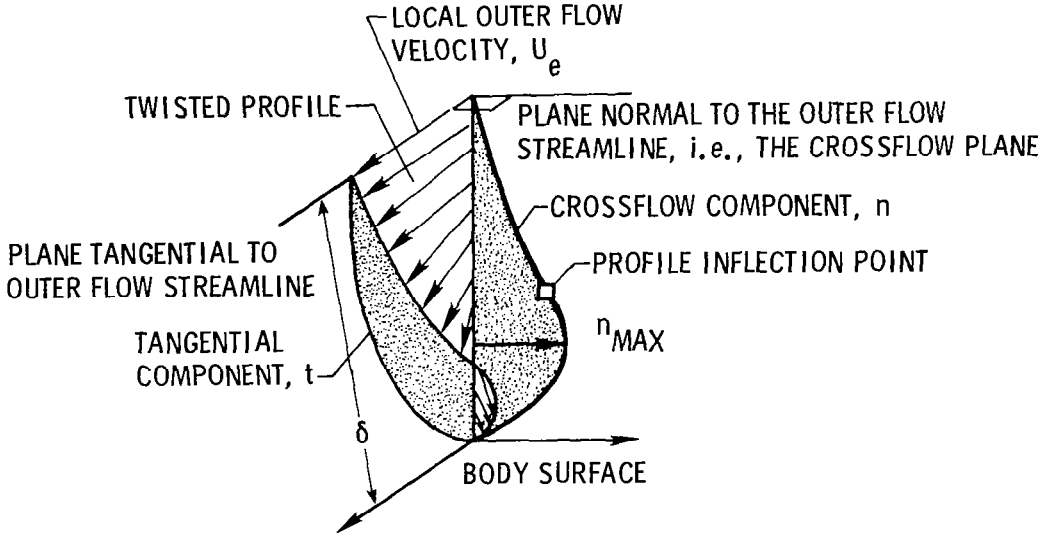

Figure 2.- Swept-wing boundary-layer profiles.

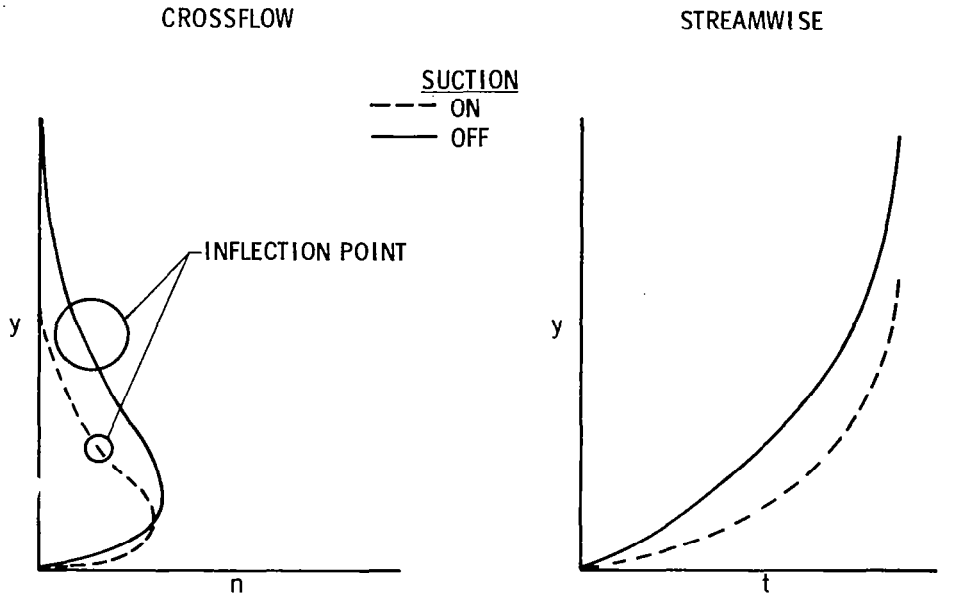

Figure 3.- Effects of suction on streamwise and crossflow boundary-layer profiles.

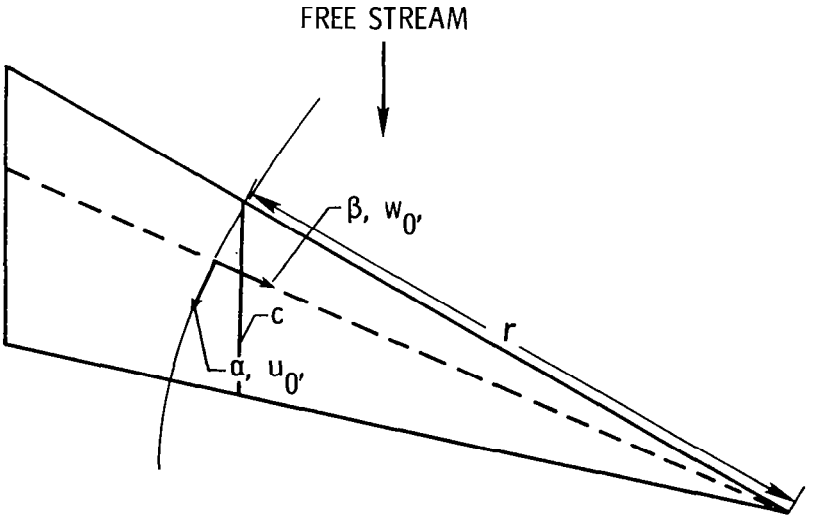

Figure 4.- Coordinates for wing boundary-layer solutions.

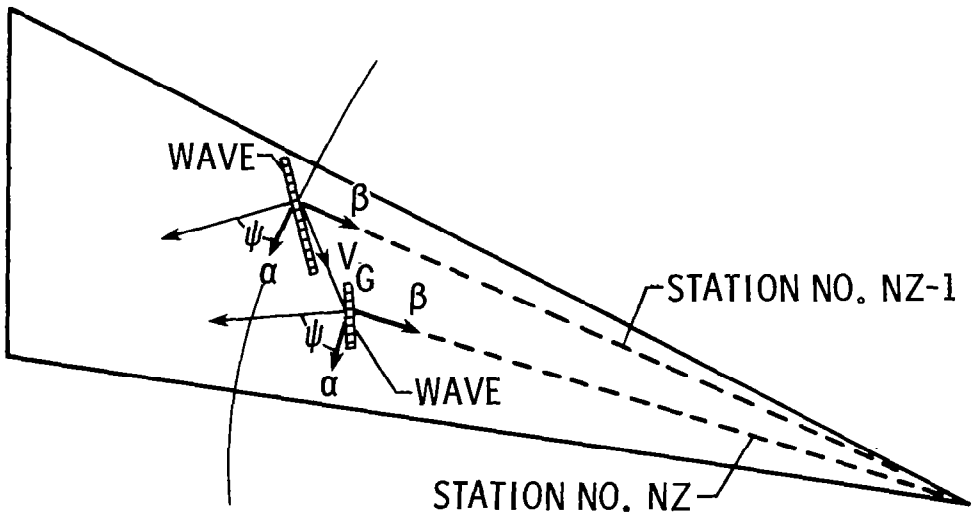

Figure 5.- Schematic of stability code integration path.

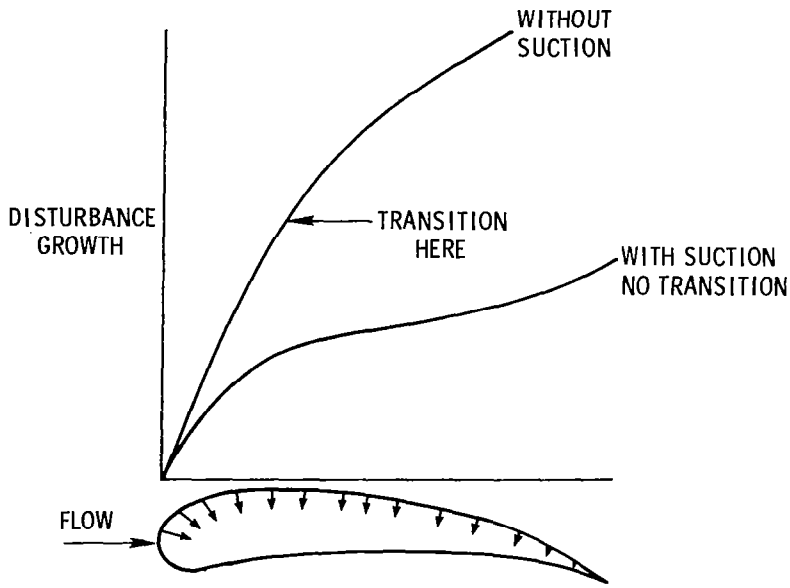

Figure 6.- Illustration of effect of suction on disturbance growth.

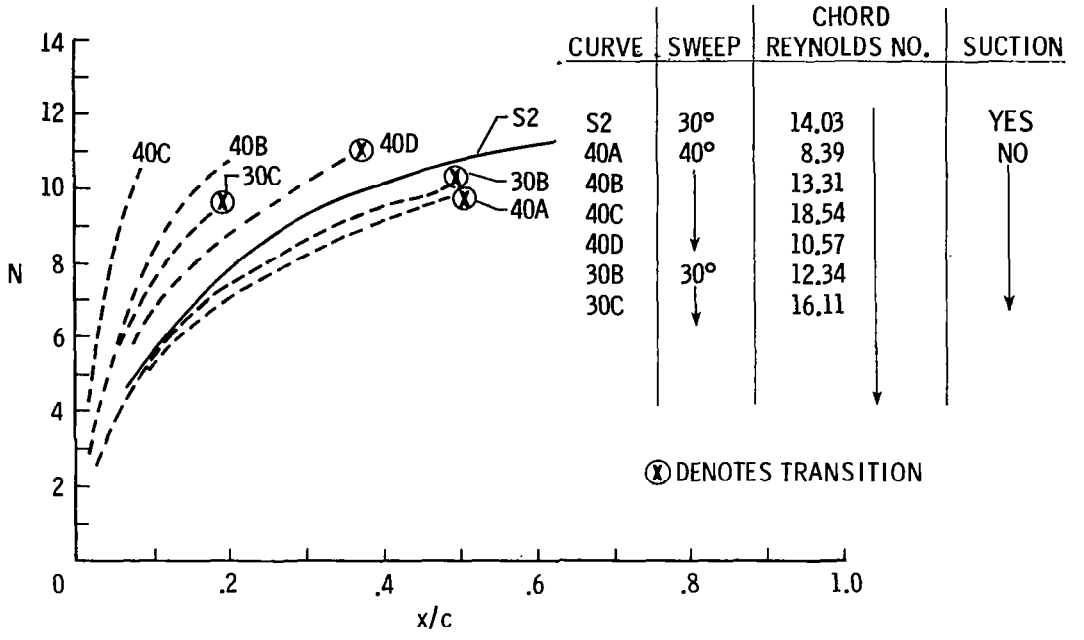

Figure 7.- Integrated "N factors" for stationary crossflow disturbances. (Front part of wing.)

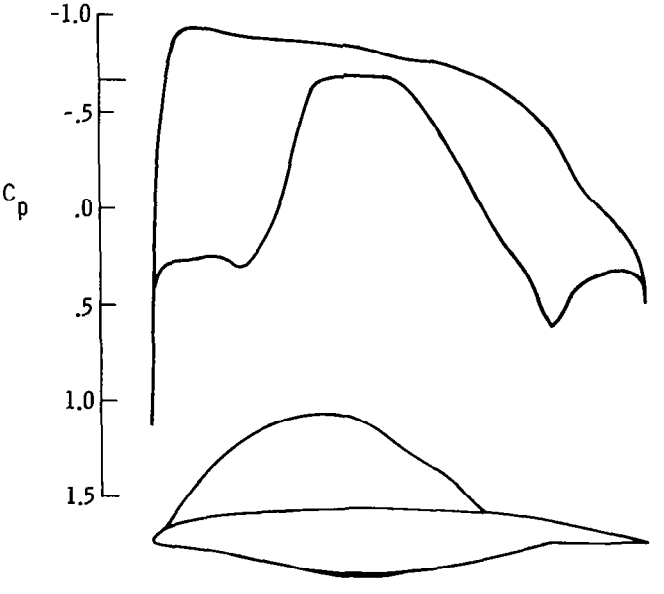

Figure 8.- Laminar flow control applicable supercritical wing section.

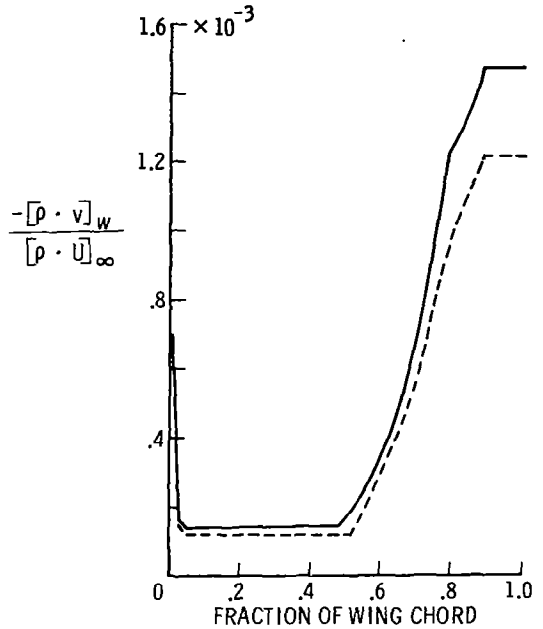

Figure 9.- Suction distributions on upper surface of wing of figure 8.

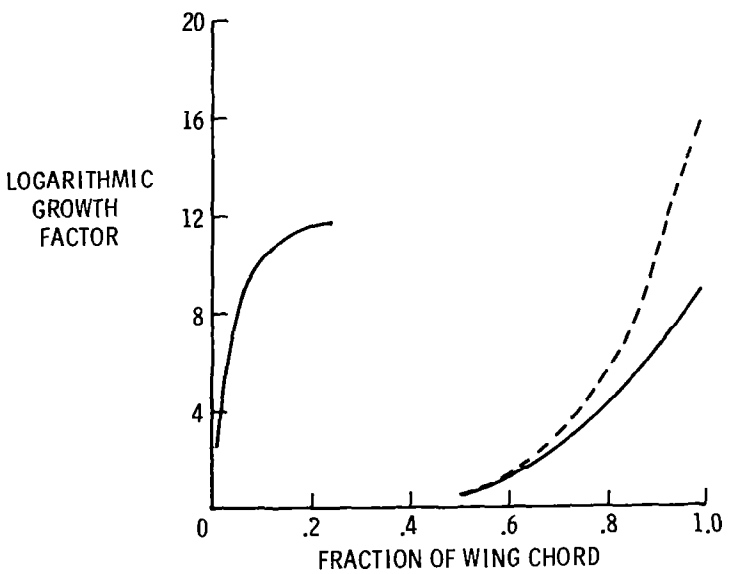

Figure 10. Integrated disturbance growth for upper surface crossflow corresponding to suction distributions of figure 9.

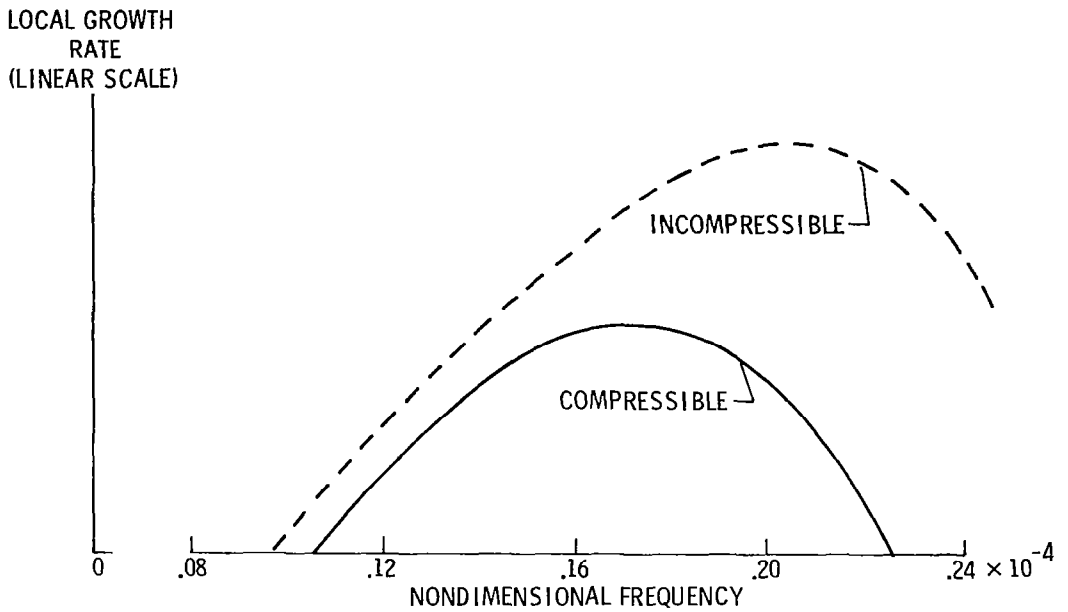

Figure 11.- Effect of compressibility on streamwise (Tollmien-Schlichting) growth rates and frequencies in upper surface supercritical region.

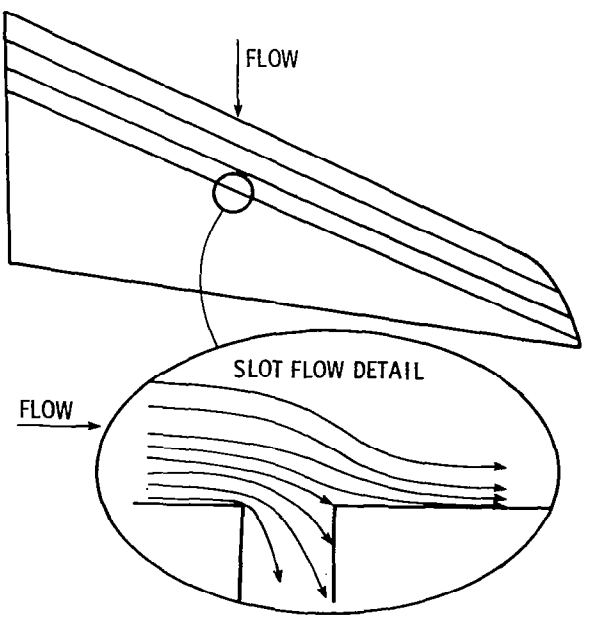

Figure 12.- Nonparallel flow near a slot.

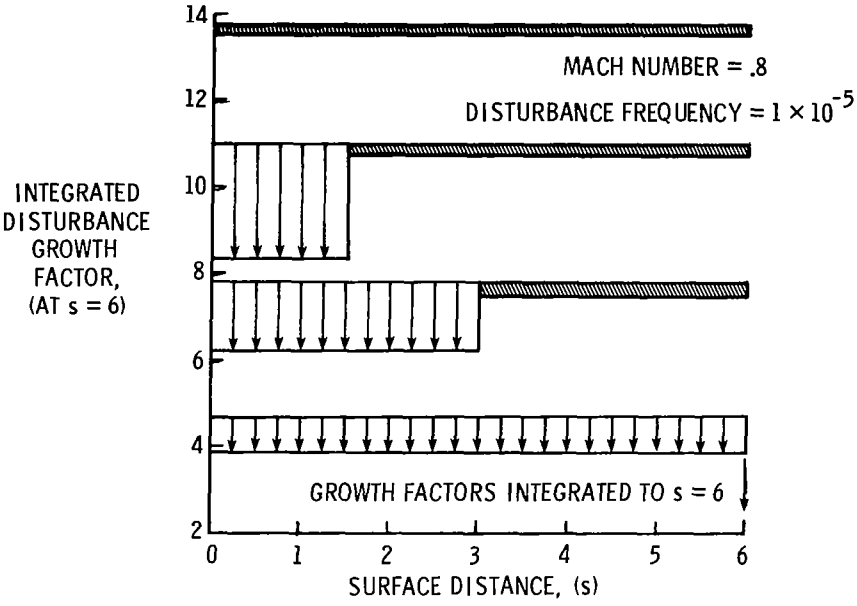

Figure 13.- Example of nonparallel disturbance growth calculation over a flat plate. Total suction fixed; distribution varied.

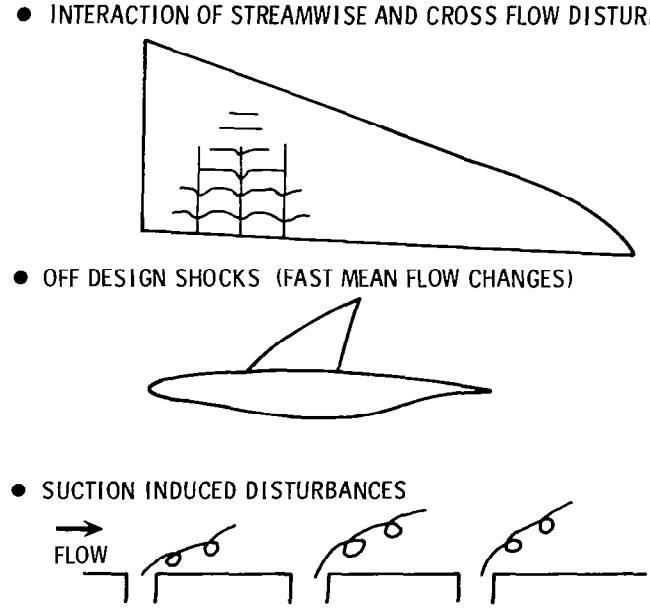

Figure 14.- Illustration of conditions for which nonlinear effects may be important.